

UDC 531.7:62-2:629.7 (043.3)

**Artur Zaporozhets**, Dr. Sci. (Engin.), Senior Researcher, <https://orcid.org/00000-0002-0704-4116>  
**Denys Kataiev\***, <https://orcid.org/0000-0002-2383-3123>  
General Energy Institute of NAS of Ukraine, 172, Antonovycha St., Kyiv, 03150, Ukraine  
\*Corresponding author: [kataev\\_d.a@ukr.net](mailto:kataev_d.a@ukr.net)

---

## METHOD OF COMPENSATING FOR INSTRUMENTAL UNCERTAINTY IN MEASUREMENTS USING A COORDINATE MEASURING ARM

**Abstract.** *Due to the influence of dynamic factors in various measurement configurations, the degree of uncertainty in measurements using a Coordinate Measuring Arm (CMA) is directly related to the measurement configuration. However, existing models for compensating CMA errors do not account dynamic factors, which impose certain limits for improving the accuracy of CMAs. To solve this issue, a method for residual error correction based on a polynomial model for single-point measurements was proposed. The influence of the CMA configuration on the residual probe error was analyzed. To enhance accuracy, a polynomial model has been developed by studying the relationship between the rotation angles of the CMA's moving elements and the probe coordinates in a cylindrical coordinate system. Experimental results demonstrate that the residual error correction method significantly compensates for instrumental uncertainty, greatly improving the accuracy of measurements using CMAs.*

**Keywords:** coordinate measuring arm, measurement error, coordinate measurements, calculation method, single-point residual correction, compensation.

### 1. Introduction

Development of scientific methods and standardization of procedures for assessing the accuracy of measurements using coordinate measuring arms (CMAs) is of utmost importance to enhance the quality and efficiency of production in the energy industry and various other sectors. These devices have become indispensable in the manufacturing of energy-related equipment due to their simple design, easy transportability, and high operational flexibility, as extensively discussed in references [1–2]. It has been demonstrated [3] that the introduction of CMAs into the energy sector allows for the modernization of metrological support by eliminating the need for designing and producing complex and metal-intensive measuring equipment, thus enabling the reverse engineering of components. Scientific research and methods for compensating measurement errors using CMAs have become an integral part of the energy equipment manufacturing process, aiming to ensure the highest quality and safety.

The precision of measurements made with CMAs is influenced by both static and dynamic factors. Static factors pertain to predictable errors arising from deviations between actual and theoretical parameters and can be mitigated through error compensation methods such as structure parameter modeling [5], calibration, and error compensation. On the other hand, dynamic factors are associated with errors arising from elastic deformation, inertia, weight in connections, thermal deformation, gaps between connections, and rebound. To compensate for these dynamic factors, it is necessary to explore the nonlinear relationships between various errors affecting measurement accuracy and consider their influence on the instrumental component of measurement uncertainty.

However, isolating individual errors can be challenging, necessitating the consideration of all factors together. In the case of CMAs, configuration is determined by motion parameters, including the lengths of struts and encoder values in different connections. Typically, dynamic factors of CMAs can be linked to the configuration defined by encoder values in all connections [8, 9].

If encoder readings are known, compensating for dynamic factor errors in different CMA configurations can be determined through system modeling [10]. Guided by these findings, the relationship between the bending angles of the arm and probe coordinates has been investigated. To improve the effectiveness of residual error correction, a triangular measurement arm model has been explored in reference [11], taking into account the peculiarities of CMAs with an adjacent orthogonal joint design. Additionally, the impact of compensating dynamic factors on the instrumental component of measurement uncertainty has been considered, contributing to the enhancement of measurement quality in various applications, particularly in the production of energy-related equipment.

## 2. Methods and material

A method for correcting the residual error of Coordinate Measuring Arms (CMAs) based on a single-point position configuration has been developed. As an example, a 6-element measuring system is used (Figure 1(a)), the configuration of which is determined by the angles of all connecting elements of the system (Figure 1(b)), and the position matrix  $P$  can be expressed by formula (1):

$$P = \prod_{j=1}^n A(\theta_j), \quad (1)$$

where  $A(\theta_j)$  is the Denavit-Hartenberg parameter matrix for the  $j$ -th connecting element, determined by the angle value  $\theta_j$  of this connecting element [15].

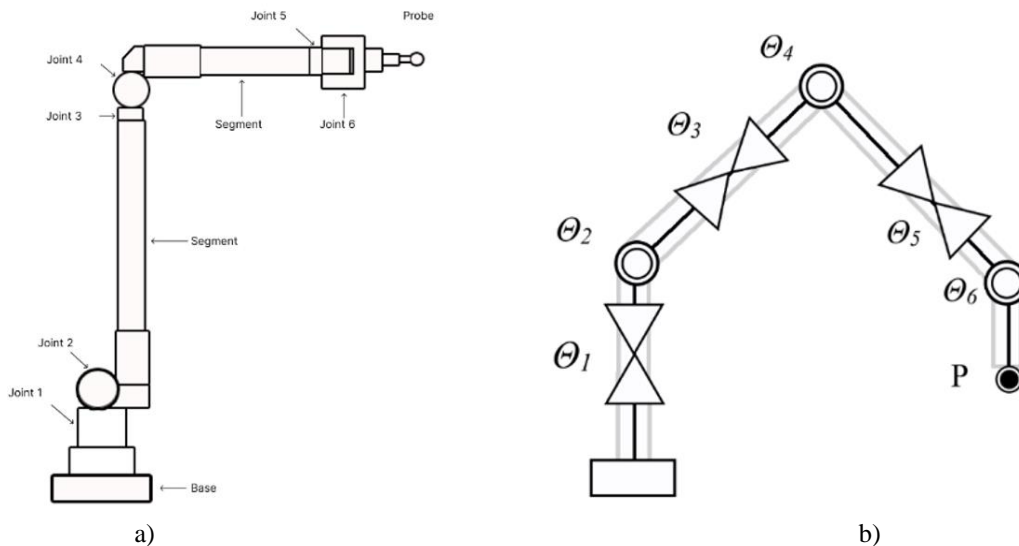


**Fig. 1.** Configuration of the 6-element measuring system

Since the terminal connecting elements of the CMA, which include the fifth and sixth connecting elements, have small length and mass, their influence on the system can be ignored [16]. The primary quality elements of the CMA are the structural elements from the second to the fourth connecting element, which are essential components leading to a certain regularity in the accuracy of the CMA in various positional configurations.

In conclusion, the relationship between the angles of the connecting elements ( $\theta_1$ ,  $\theta_2$ ,  $\theta_3$ ) and the probe coordinates exists in the residual error correction [17].

Investigation of the relationships between the angles of the CMA segment connections and the probe coordinates.

As shown in Figure 1b, a set of configurations is established when the position of the CMA probe with the first four connecting elements ( $\theta_1, \theta_2, \theta_3$ ) is determined. In theory, the set of configurations can be located on the boundary of a circle referred to as the configuration circle [18].

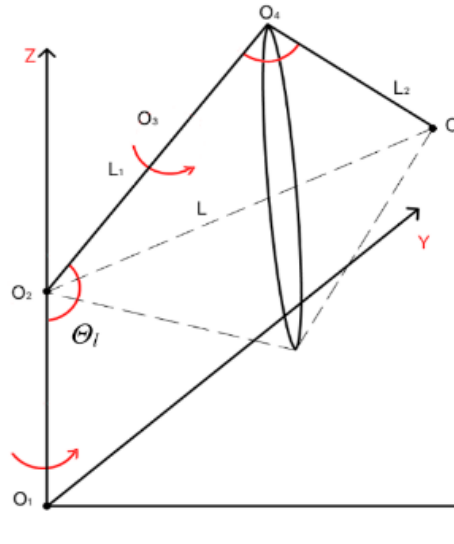


**Fig. 2.** CMA configuration circle (diagram of CMA element placement)

The coordinates of the connection point  $O_5 (x_{O_5}, y_{O_5}, z_{O_5})$  can be calculated using the inverse solution of the Denavit-Hartenberg parameter matrix, as described in [12]. With the position of  $O_5 (x_{O_5}, y_{O_5}, z_{O_5})$  you can calculate the coordinates of  $O_2 (x_{O_2}, y_{O_2}, z_{O_2})$ , the lengths  $L_1, L_2$ , and the distance between  $O_2$  and  $O_5$ , denoted as  $L$ , using formula (2) [19]:

$$L = \sqrt{(x_{O_2} - x_{O_5})^2 + (y_{O_2} - y_{O_5})^2 + (z_{O_2} - z_{O_5})^2}. \quad (2)$$

The value of the angle  $\theta_4$  for the fourth connection can be calculated using formula (3):

$$\cos \theta_4 = \frac{L_1^2 + L_2^2 - L^2}{2L_1L_2}. \quad (3)$$

According to formulas (2) and (3), the position of the triangle  $\Delta O_2 O_4 O_5$  in the coordinate system  $O_1 (x, y, z)$  can be determined using the angle  $\theta_3$  of the third connecting element and the angle  $\theta_1$  between the Z-axis and the linear segment  $O_2 O_5$ [20]. As shown in Figure 1b, the angle  $\theta_1$  can be calculated using formulas (4), (5) and (6):

$$\theta_1 = \pi - \arccos \left( \frac{|ab|}{|a||b|} \right), \quad (4)$$

$$a = O_i + O_j + z_{O_2} k, \quad (5)$$

$$b = (x_{O_5} - x_{O_2})i + (y_{O_5} - y_{O_2})j + (z_{O_5} - z_{O_2})k, \quad (6)$$

where  $a$  is the vector in the direction of the Z-axis;  $b$  is the vector in the direction of the segment  $O_2 O_5$ .

Typically, the Z-axis is perpendicular to the horizontal plane.

Let's consider the dynamic deformation of the CMA as parameters  $\Delta z, \Delta s$  i  $\Delta h$ . As shown in Figure 3,  $\Delta z$  represents the deformation along the Z-coordinate of  $O_5$ ;  $\Delta s$  represents the tangential deformation of the  $O_5$  coordinate in the XY plane, and  $\Delta h$  represents the radial deformation of the  $O_5$  in the XY plane [21]. ( $\Delta z, \Delta s, \Delta h$ ) can be referred to as residual errors in the cylindrical coordinate system of the CMA, which are discrepancies between theoretical and practical values [22].

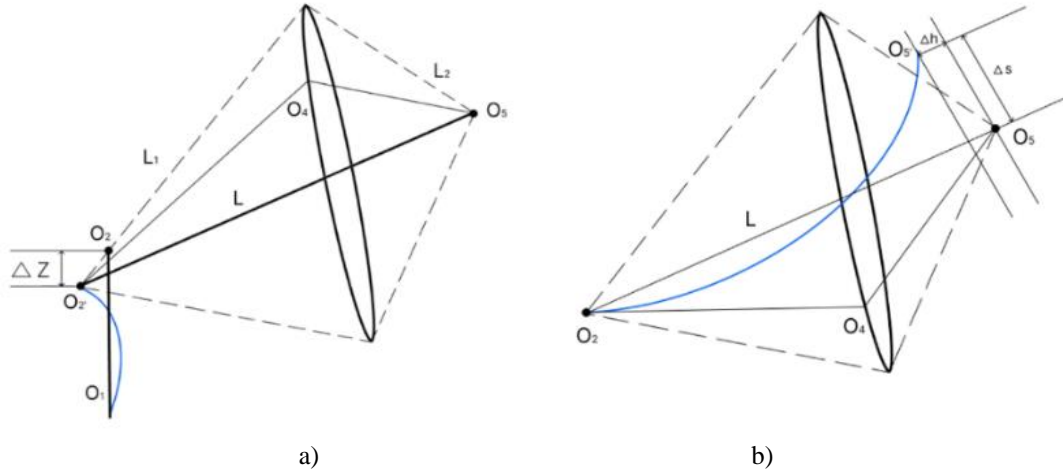


**Fig. 3.** Front view of deformation (a), Top view of deformation (b)

So, the position configuration depends on  $\theta_3$ ,  $\theta_4$  and  $\theta_l$ ; and the mapping relationship between  $(\theta_3, \theta_4, \theta_l)$  and  $(\Delta z, \Delta s, \Delta h)$  can be expressed using (7):

$$(\theta_3, \theta_4, \theta_l) \rightarrow (\Delta z, \Delta s, \Delta h). \quad (7)$$

To calculate the residual correction, the polynomial equation (8) can be used to approximate (7):

$$\begin{aligned} \Delta z &= k_{z_0} + \sum_{i=0}^2 \left( k_{z_{(1+3i)}} \theta_3^i \theta_4^{2-i} + k_{z_{(2+3i)}} \theta_4^i \theta_l^{2-i} + k_{z_{(3+3i)}} \theta_l^i \theta_3^{2-i} \right), \\ \Delta s &= k_{s_0} + \sum_{i=0}^2 \left( k_{s_{(1+3i)}} \theta_3^i \theta_4^{2-i} + k_{s_{(2+3i)}} \theta_4^i \theta_l^{2-i} + k_{s_{(3+3i)}} \theta_l^i \theta_3^{2-i} \right), \\ \Delta h &= k_{h_0} + \sum_{i=0}^2 \left( k_{h_{(1+3i)}} \theta_3^i \theta_4^{2-i} + k_{h_{(2+3i)}} \theta_4^i \theta_l^{2-i} + k_{h_{(3+3i)}} \theta_l^i \theta_3^{2-i} \right), \end{aligned} \quad (8)$$

where  $k_{z_j}$ ,  $k_{s_j}$ ,  $k_{h_j}$  are the coefficients of the polynomial [23].

The method for constructing a residual correction model consists of the following stages:

1. Data Collection: In the measurement space of the CMA, the horizontal plane of the base is taken as a reference, and several positions within the range of 20–80 % from the radial direction of CMA measurements (Figure 3) are selected. In these locations, data is collected from a single point using the method illustrated in Figure 4. Data for  $\theta_3$  and  $\theta_4$ , which are the values of the CMA's connections  $O_3$  and  $O_4$  can be obtained from encoders. The probe coordinates and  $L$  can be calculated using equations (1) and (4), respectively [24].
2. Calculation of Residual Values: The average values  $(\bar{x}, \bar{y}, \bar{z})$  and the coordinates of a single point  $(x_i, y_i, z_i)$  are used as initial data [25]. Then  $(\Delta z_i, \Delta s_i, \Delta h_i)$  can be expressed using formula (9):

$$\begin{aligned} \Delta z_i &= z_i - \bar{z}, \\ \Delta s_i &= \sqrt{x_i^2 + y_i^2} \sin \theta_i, \\ \Delta h_i &= \sqrt{x_i^2 + y_i^2} \cos \theta_i - \sqrt{\bar{x}^2 + \bar{y}^2}, \theta_i = \arctan \frac{\bar{y}}{\bar{x}} - \arctan \frac{y_i}{x_i}. \end{aligned} \quad (9)$$

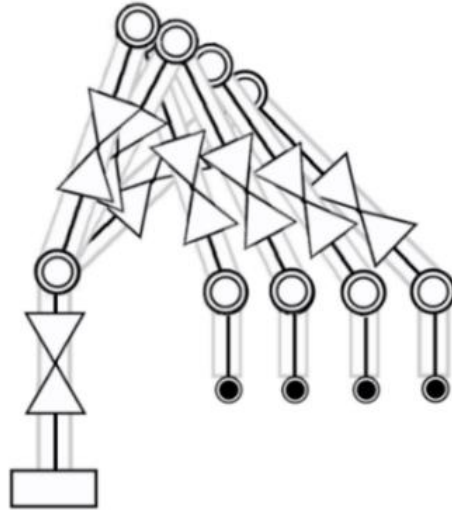


**Fig. 4.** Determining the single-point position

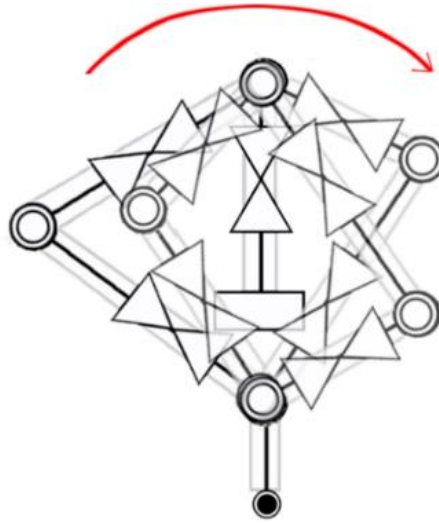


**Fig. 5.** Sequence of positioning for determining single-point position

3. According to (8), the residual correction equations can be established along with  $(\theta_3, \theta_4, \theta_l)$  and  $(\Delta z_i, \Delta s_i, \Delta h_i)$ . The polynomial coefficients  $(kz_j, ks_j, kh_j)$  can be calculated using the residual correction equations.
4. Compensation Calculation: To enhance the accuracy of the CMA, the compensation values  $(\Delta x_i, \Delta z_i, \Delta y_i)$  for the coordinate  $(x_i, y_i, z_i)$  of the probe should be computed using the method of residual value correction. According to the relationship between the cylindrical coordinate system and Cartesian coordinates, the compensation values can be calculated using the equation.

$$\begin{cases} \Delta x_i = |\Delta h_i| \cos \theta_i + |\Delta s_i| \sin \theta & (\Delta s_i \geq 0), \\ \Delta x_i = |\Delta h_i| \cos \theta_i - |\Delta s_i| \sin \theta & (\Delta s_i < 0) \\ \Delta y_i = |\Delta s_i| \cos \theta_i + |\Delta h_i| \sin \theta & (\Delta h_i \geq 0) \\ \Delta y_i = |\Delta s_i| \cos \theta_i - |\Delta h_i| \sin \theta & (\Delta h_i < 0) \end{cases} \quad (10)$$

$$x = x_i - \Delta x_i \qquad x = x_i + \Delta x_i \quad (11)$$

$$y = y_i + \Delta y_i (x < 0); \quad y = y_i - \Delta y_i (x \geq 0); \quad z = z_i - \Delta z_i; \quad z = z_i + \Delta z_i,$$

where

$$\theta = \arctan \frac{y_i}{x_i} + \arcsin \frac{\Delta s_i}{\sqrt{x_i^2 + y_i^2}}.$$

Then, the root means square deviation (RMSD) can be calculated as (12) and (13):

$$\delta_i = \sqrt{(x_i - x_a)^2 + (y_i - y_a)^2 + (z_i - z_a)^2}, \quad (12)$$

$$S = \sqrt{\frac{\sum \delta_i^2}{(n-1)}}, \quad (13)$$

where n is the number of single-point measurements;  $(x_i, y_i, z_i)$  are the coordinates for each measurement; and;  $(x_a, y_a, z_a)$  is the mean value of measurements over n repetitions [26].

The algorithm for calculating the residual correction method is shown in Figure 6.

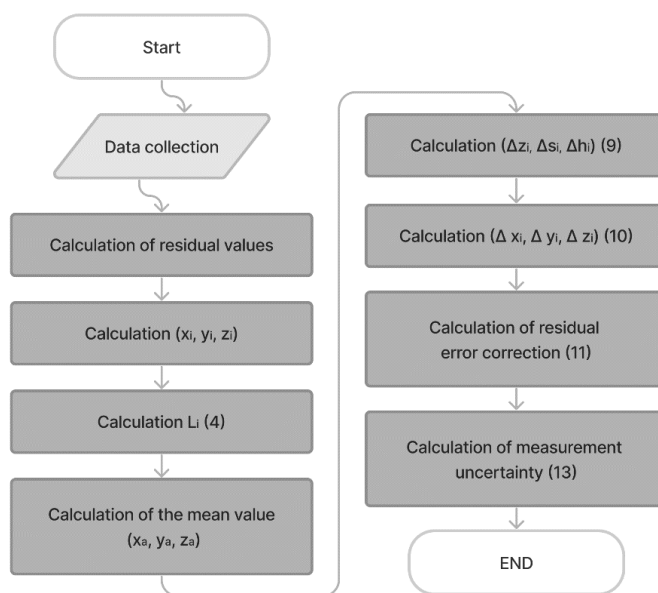


**Fig. 6.** Algorithm for calculation using the residual error correction method

The application of this method significantly reduces the instrumental component of uncertainty in measurements using CMA.

### 3. Results

Using computer modeling, correction of residual errors in single-point measurements was carried out. The structural parameters of the 6-element measurement system are provided in Table 1.

**Table 1.** Denavit-Hartenberg parameters for the 6-element measurement system

	Joint 1	Joint 2	Joint 3	Joint 4	Joint 5	Joint 6
$l_i(\text{mm})$	0	-90	90	0	0	155.479
$d_i(\text{mm})$	0	0	-650	0	-435	65.931
$a_i(\text{rad})$	-1.57	1.57	-1.57	1.57	1.57	0
$\theta_i(\text{rad})$	0	0.001	0.002	0.003	0.005	0.04

Ten single-point measurements were conducted using the method illustrated in Figure 6. The obtained results are provided in Table 2.

**Table 2.** Results of single-point measurements before applying the method

№	1	2	3	4	5	6	7	8	9	10
x	0.23	0.18	0.18	0.08	0.05	-0.12	-0.15	-0.31	-0.08	-0.09
y	0.61	0.55	0.42	0.36	0.12	-0.42	-0.48	-0.42	-0.38	-0.28
z	-0.26	-0.27	-0.33	-0.35	-0.29	-0.06	0.19	0.39	0.47	0.52

Data obtained after applying the single-point residual correction method are provided in Table 3.

**Table 3.** Results of single-point measurements after applying the method

№	1	2	3	4	5	6	7	8	9	10
x	0.09	0.01	0.02	-0.05	0.01	0.02	0.01	-0.17	0.05	0.05
y	0.09	0.05	-0.02	-0.02	-0.12	-0.09	-0.06	0.02	0.10	0.18
z	0.04	0.04	-0.01	-0.01	0.04	0.04	-0.12	-0.05	0.01	0.17

A comparative analysis of the results of computer modeling for measurements conducted before and after applying the single-point residual correction method is provided in Figure 7 (a, b).

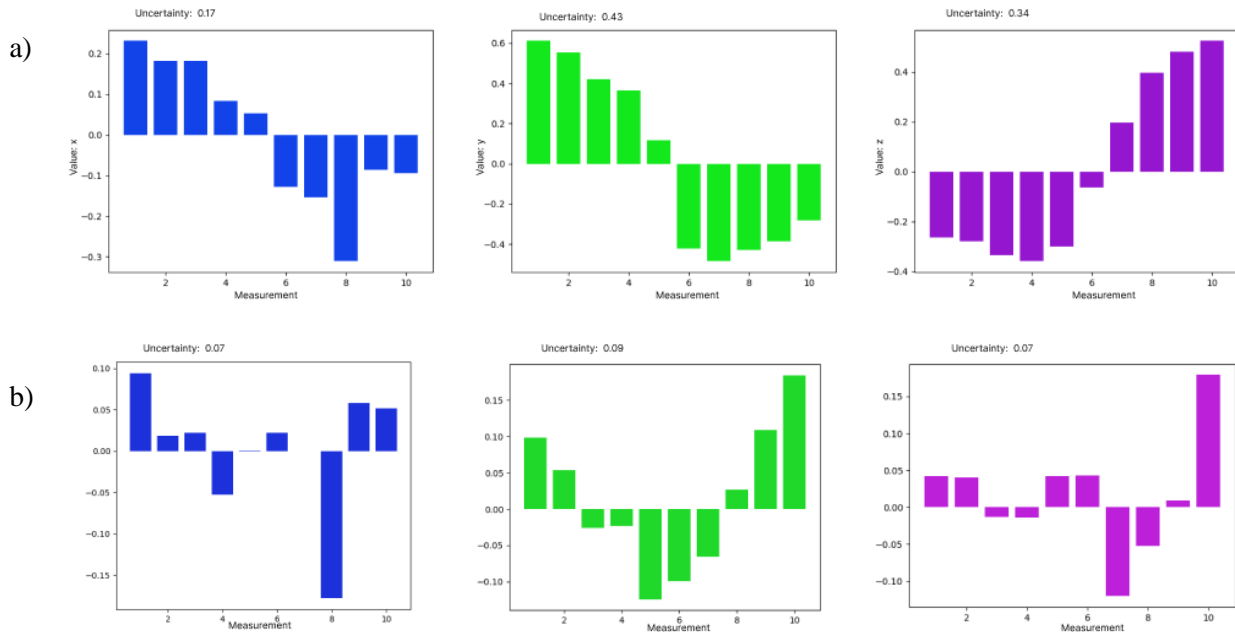


**Fig. 7.** Computer modeling before applying the single-point residual correction method (a), Computer modeling after applying the single-point residual correction method (b)

As a result, the uncertainty index of the instrumental error in measurements before applying the single-point residual correction method is 0.59, and after applying the method, it is 0.14. Therefore, the proposed method of residual value correction significantly compensates for the instrumental component of uncertainty, thus greatly improving the accuracy of measurements using CMA.

#### 4. Conclusion

The article presents a method aimed at improving the accuracy of measurements using Coordinate Measuring Arms (CMAs). This method is based on the analysis of dynamic factors that affect the accuracy of CMA measurements and considers their influence on measurement results. The impact of dynamic factors on measurement accuracy has been investigated, and a method for compensating for residual errors has been proposed. The relationship between the angles of inclination of CMA's moving elements and the probe coordinates

in a cylindrical coordinate system has been studied. Through systematic modeling, correlations between the angles of inclination of moving elements and errors affecting measurement accuracy have been established.

Experimental results have shown that the proposed method significantly enhances the accuracy of CMA measurements by reducing the instrumental component of uncertainty. Therefore, the application of the method for compensating for the instrumental component of uncertainty in measurements using CMAs represents an important step in improving measurement accuracy in various fields, including the production of energy equipment. This method can be used to reduce the influence of dynamic factors and enhance the quality and reliability of measurements using Coordinate Measuring Arms.

## References

1. Xuefeng, Y., Ci, S., Jin, Y., Lu, Y., & Hongwei, Z. (2016). Development and error compensation of the high precision turntable. *Chinese Journal of Scientific Instrument*, 37(5), 961–967.
2. Zhaorui, Z., Xu, Z., & Zelong, Z. (2015). Hand-eye calibration method fusing rotational and translational constraint information. *Chinese Journal of Scientific Instrument*, 36(11), 2443–2450.
3. Cheng, Y., Chen, X., & Wang, H. (2016). Measurement uncertainty estimation and analysis based on accuracy theory. *Journal of Electronic Measurement and Instrumentation*, 30(8), 1175–1182.
4. Cheng, Y., Wang, Z., Chen, X., Li, Y., Li, H., Li, H., & Wang, H. (2016). Evaluation and Optimization of Task-oriented Measurement Uncertainty for Coordinate Measuring Machines Based on Geometrical Product Specifications. *Applied Sciences*, 9(1), 6–15. <https://doi.org/10.3390/app9010006>
5. Tung, T. T., Tinh, N. V., Thao, D. T. P., & Minh, T. V. (2023). Development of a prototype 6 degree of freedom robot arm. *Results in Engineering*, 18. <https://doi.org/10.1016/j.rineng.2023.101049>
6. Wen, Z. M., Wang, Y. J., & Di, N. (2014). On-orbit hand-eye calibration using cooperative target. *Chinese Journal of Scientific Instrument*, 35(5), 1005–1012.
7. Zhuang, J., Wang, B., & Xiang, M. (2015). Application of MEMS IMU random error modeling in SAR motion compensation. *Foreign Electronic Measurement Technology*, 34(10), 88–94.
8. Rongsheng, L., Wanhong, L., & Dabao, L. (2014). Angular error compensation for laser tracker. *Optics and Precision Engineering*, 22(9), 2299–2305. <http://doi.org/10.3788/OPE.20142209.2299>
9. Wang, Y., Xue, Z., Huang, Y., & Wang, X. (2016, January 26). Study on self-calibration angle encoder using simulation method. *Seventh International Symposium on Precision Mechanical Measurements*, 9903. <https://doi.org/10.1117/12.2217638>
10. You, X., Huiyuan, X., & Zhijian, Z. (2011). Single-point residual correction method for multi-joint arm based on pose configuration. *Chinese Journal of Scientific Instrument*, 32(4), 775–780. <https://doi.org/10.1177/1729881420925638>
11. Huiyuan, X., You, X., & Zhijian, Z. (2012). The multi-joint measuring arm's error compensation method based on the pose configurations. *Applied Mechanics and Materials*, 117-119, 751–755. <https://doi.org/10.4028/www.scientific.net/amm.117-119.751>
12. Lopez-Franco, C., Hernández-Barragán, J., Alanis, A. Y., Arana-Daniel, N., & López-Franco, M. (2018). Inverse kinematics of mobile manipulators based on differential evolution. *International Journal of Advanced Robotic Systems*, 15(1), 27–38. <https://doi.org/10.1177/1729881417752738>
13. Bing, H., Linxian, C., & Chusheng, L. (2014). Complex differential evolution algorithm for inverse kinematics of spatial 6R robot manipulators. *Journal of Mechanical Engineering*, 50(15), 45–52. <http://www.cjmenet.com.cn/CN/Y2014/V50/I15/45>
14. Liao, Z., Tang, S., & Wang, D. (2023). A New Kinematic Synthesis Model of Spatial Linkages for Designing Motion and Identifying the Actual Dimensions of a Double Ball Bar Test Based on the Data Measured. *Machines*, 11(9), 919. <https://doi.org/10.3390/machines11090919>
15. Asmai, E., Hennebelle, F., & Coorevits, T. (2018). Rapid and robust on-site evaluation of articulated arm coordinate measuring machine performance. *Measurement Science and Technology*, (29), 1–14. <https://doi.org/10.1088/1361-6501/aade10>
16. Cheng, W., Yu, L., & Fei, Y. (2011). Study on parameter identification algorithms for articulated arm coordinate measuring machine. *University Science Technology China*, (41), 45–49.
17. Gao, G., Zhang, H., & Guo, Y. (2016). Structural Parameter Identification of Articulated Arm Coordinate Measuring Machines. *Mathematical Problems in Engineering*, (3), 1–10. <https://doi.org/10.1155/2016/4063046>

18. Huang, J., Cao, Y., & Xiong, C. (2018). An echo state Gaussian process-based nonlinear model predictive control for pneumatic muscle actuators. *IEEE Transactions on Automatic Control*, 16(3), 1071–1084. <https://doi.org/10.1109/TASE.2018.2867939>
19. Gao, G., Sun, G., & Na, J. (2018). Structural parameter identification for 6 DOF industrial robots. *Mechanical Systems and Signal Processing*, 113, 145–155. <https://doi.org/10.1016/j.ymssp.2017.08.011>
20. Luo, Z., Liu, H., & Li, D. (2018). Analysis and compensation of equivalent diameter error of articulated arm coordinate measuring machine. *Measurement and Control*, 51(5), 16–26. <https://doi.org/10.1177/0020294018755324>
21. Zhou, Z., Guo, H., Wang, Y., & Liu, X. (2018). Inverse kinematics solution for robotic manipulator based on extreme learning machine and sequential mutation genetic algorithm. *International Journal of Advanced Robotic Systems*, 15(4), 1–15. <https://doi.org/10.1177/1729881418792992>
22. Huang, J., Ri, S., & Fukuda, T. (2019). A disturbance observer based sliding mode control for a class of underactuated robotic system with mismatched uncertainties. *IEEE Transactions on Automatic Control*, 64(6), 2480–2487. <https://doi.org/10.1109/tac.2018.2868026>
23. Gao, G., Zhang, H., & San, H. (2019). Kinematic calibration for industrial robots using articulated arm coordinate machines. *International Journal of Modelling, Identification and Control*, 31(1), 16–26. <https://doi.org/10.1504/ijmic.2019.096816>
24. Gao, G., Zhao, J., & Na, J. (2018). Decoupling of kinematic parameter identification for articulated arm coordinate measuring machines. *IEEE Access*, 6(50), 433–442. <https://doi.org/10.1109/access.2018.2868497>
25. Wan, L., Sun, Y., & Zhang, H. (2019). Global fast terminal sliding mode control based on radial basis function neural network for course keeping of unmanned surface vehicle. *International Journal of Advanced Robotic Systems*, 16(2), 1–12. <https://doi.org/10.1177/1729881419829961>
26. Park, B., Pedrycz, W., & Oh, S. (2010). Polynomial-based radial basis function neural networks (P-RBF NNs) and their application to pattern classification. *Applied Intelligence*, 32, 27–46. <https://doi.org/10.1007/s10489-008-0133-z>

## МЕТОД КОМПЕНСАЦІЇ ІНСТРУМЕНТАЛЬНОЇ СКЛАДОВОЇ НЕВИЗНАЧЕНОСТІ ПРИ ВИМІРЮВАННЯХ ІЗ ЗАСТОСУВАННЯМ КООРДИНАТНО-ВИМІРЮВАЛЬНОЇ РУКИ

Артур Запорожець, д-р техн. наук, ст. досл., <https://orcid.org/00000-0002-0704-4116>

Денис Катаєв\*, <https://orcid.org/0000-0002-2383-3123>

Інститут загальної енергетики НАН України, вул. Антоновича, 172, м. Київ, 03150, Україна

\*Автор-кореспондент: [kataev\\_d.a@ukr.net](mailto:kataev_d.a@ukr.net)

**Анотація.** У зв'язку з впливом динамічних факторів у різних конфігураціях вимірювання ступінь невизначеності при вимірюваннях за допомогою координатно-вимірювальної руки (КВР) безпосередньо пов'язаний з конфігурацією вимірювання. Однак існуючі моделі компенсації похибок КВР не враховують динамічні фактори, що встановлює певні межі підвищення точності КВР. Для вирішення цієї проблеми було запропоновано метод коригування залишкової похибки на основі поліноміальної моделі для одноточкових вимірювань. Проаналізовано вплив пози конфігурації КВР на залишкову помилку зонда. Для підвищення точності пропонується поліноміальна модель, що була визначена шляхом вивчення зв'язку між кутами повороту рухомих елементів КВР та координатами зонда в циліндричній системі координат. Експериментальні результати показують, що метод корекції залишкових значень дозволяє істотно компенсувати інструментальну складову невизначеності, що суттєво покращує точність вимірювань за допомогою КВР.

**Keywords:** координатно-вимірювальна рука, похибка вимірювання, координатні вимірювання, метод розрахунку, одноточкова корекція залишкових значень, компенсація.

Надійшла до редколегії: 08.11.2023